Dynamics of the Nucleotide Pocket of Myosin Measured by Spin-Labeled Nucleotides

Nariman Naber,* Thomas J. Purcell,*[†] Edward Pate,[‡] and Roger Cooke*[†]

*Department of Biochemistry and Biophysics and [†]Cardiovascular Research Institute, University of California, San Francisco, California 94158; and [‡]Department of Pure and Applied Mathematics, Washington State University, Pullman, Washington 99164

ABSTRACT   We have used electron paramagnetic probes attached to the ribose of ATP (SL-ATP) to monitor conformational changes in the nucleotide pocket of myosin. Spectra for analogs bound to myosin in the absence of actin showed a high degree of immobilization, indicating a closed nucleotide pocket. In the Actin·Myosin·SL-AMPPNP, Actin·Myosin·SL-ADP·BeF₃, and Actin·Myosin·SL-ADP·AlF₄ complexes, which mimic weakly binding states near the beginning of the power stroke, the nucleotide pocket remained closed. The spectra of the strongly bound Actin·Myosin·SL-ADP complex consisted of two components, one similar to the closed pocket and one with increased probe mobility, indicating a more open pocket, The temperature dependence of the spectra showed that the two conformations of the nucleotide pocket were in equilibrium, with the open conformation more favorable at higher temperatures. These results, which show that opening of the pocket occurs only in the strongly bound states, appear reasonable, as this would tend to keep ADP bound until the end of the power stroke. This conclusion also suggests that force is initially generated by a myosin with a closed nucleotide pocket.

INTRODUCTION

Myosin produces force in a cyclic interaction in which it binds to actin, executes a power stroke, and is released by the binding of ATP (1–6). Hydrolysis of the nucleotide allows the Myosin·ADP·Pi complex to rebind weakly to actin, which promotes the release of phosphate. After phosphate release, the affinity of Myosin·ADP for actin increases by about a factor of 10^3 with ADP subsequently released near the end of the power stroke. Thus, in this cycle of interactions, two ligands, actin and nucleotide, compete sequentially and antagonistically for binding to myosin. The binding of actin promotes the release of nucleotide, and the binding of nucleotide weakens the interaction with actin. The conformational changes in myosin that are responsible for producing the communication between the binding of actin and nucleotides are currently a focus of investigation. In this article, we investigate this communication by measuring the conformation of the nucleotide pocket of myosin as a function of the nucleotide at the active site and binding of actin to the Myosin·Nucleotide complex.

The initial x-ray structures of myosin showed the nucleotide triphosphate moiety to be tightly encased in a narrow tunnel (7). This ''phosphate tube'' has three conserved structural components, the P-loop sequence, diagnostic for ATPases, and regions topologically homologous to switch 1 and switch 2 in the G-proteins (8–10). We experimentally demonstrated that nucleotide analogs with moieties attached to the γ-phosphate position of ATP that were too large to fit through the phosphate tube still bound to myosin. This result

proved that the phosphate tube had to open, which was the only way these analogs could bind (11). The ability of these analogs to bind to myosin was further promoted by the binding of actin, showing that the nucleotide pocket was more easily opened in the presence of bound actin (see Discussion). Structural similarities suggest that myosin, kinesin-family motors, and the G-proteins have evolved from a common ancestor protein (12). The motivation for our original line of inquiry was the observation that in the crystal structures of kinesin-family motors, switch 1 was displaced from the nucleotide triphosphates, opening the phosphate tube and leaving the triphosphate moiety exposed to solvent (13). In the G-protein family, switch 1 is seen in both the open and closed positions (10). This led us to propose that the opening of the nucleotide site in myosin was the result of a displacement of switch 1. Further support for this hypothesis came from our subsequent observations that a modeled closed switch 1 in a kinesin-family motor based on the closed switch 1 of myosin remained stably closed in molecular dynamics simulations (14) and yielded modeled probe mobilities consistent with experimental observations for spin-labeled nucleotides bound to the microtubule motors, kinesin, and ncd (15,16). Here we extend these protocols using spin-labeled nucleotides bound to myosin and actomyosin to further probe the opening and closing of the nucleotide site of myosin.

Recent crystal structures and reconstructions of electron micrographs of actomyosin complexes have both shown the myosin nucleotide pocket in an open form. Myosin V has a closed phosphate tube with bound ADP·BeF₃ and a very open nucleotide pocket, both in the absence of nucleotides and in the presence of bound ADP (17,18). The more open nucleotide pocket was the result of a displacement of switch 1 away from the triphosphates because of the movement of the

upper 50 kDa domain that was likewise coupled with the closing of the prominent actin-binding cleft in myosin. The actin-binding cleft originates near the γ-phosphate position of the bound nucleotide and spans the 5-nm distance to the actin binding site on myosin. A currently popular hypothesis is that the opening and closing of the actin-binding cleft could provide a route of communication between the binding site of actin and nucleotide. Additional structures with open nucleotide pockets were observed in the *Dictyostelium* myosin II motor domain (19) and in myosin VI (20). The myosin VI crystal structure shows that a unique insert modulates nucleotide pocket accessibility and switch 1 flexibility, allowing the insert to alter nucleotide kinetics. This is consistent with a critical role for switch 1 in regulating the affinity for nucleotide in various myosin and actomyosin states. The closing of the actin-binding cleft allows the myosin crystal structures to dock well into electron microscopy-based models of the structure of the actomyosin complex (21–23). Spectroscopic data have also shown changes in the actin-binding cleft on binding to actin (24–27) and changes in the conformation of the nucleotide pocket (26,28–31). Together these data suggest that the myosin nucleotide site can exist in both open and closed conformations. When myosin is bound strongly to actin, the nucleotide pocket is in an open conformation with the actin-binding cleft closed.

We have used EPR spectroscopy of spin probes attached to nucleotides to monitor changes in the conformation of the nucleotide site of rabbit skeletal myosin. EPR spectroscopy has proven to be a powerful method for monitoring conformational changes in proteins. Spin-labeled nucleotides have been shown to be reasonable substrates supporting muscle tension and velocity that are within a factor of 2 of that produced by ATP (32,33). EPR has the advantage that conformational changes can be measured under physiological conditions in both the presence and absence of actin. In many cases multiple conformations can be resolved, which, along with a series of spectra at different temperatures, allows one to measure the thermodynamic parameters associated with the transition between the conformations. Nucleotide-analog EPR spin probes allow us to place a reporter group at the nucleotide site. Here we use spin-labeled nucleotides to monitor the conformation of the nucleotide site of myosin, in different nucleotide- and actin-bound states. We find that the nucleotide site is predominantly in a closed form in the absence of actin. It remains predominantly in this closed form when myosin is bound to actin in states that mimic those that are thought to occur near the beginning of the power stroke, e.g., Actin·Myosin·ADP·Pi or Actin·Myosin·ATP. When myosin is bound to actin in the strong state, Actin·Myosin·ADP, found near the end of the power stroke, the nucleotide pocket is in an equilibrium between open and closed forms, with the open form favored at higher temperatures. We conclude that the energetic differences between open and closed forms of the nucleotide pocket are not great in the strongly bound Actin·Myosin·SL·ADP state.

METHODS

Protein preparations

Rabbit skeletal myosin and α-chymotryptic S1 were prepared as described previously (34). F-actin was purified from rabbit skeletal muscle (35). Rabbit fibers, both fast (psoas) and slow (soleus or semimembranosus), were harvested and chemically skinned as described previously (36). Minced muscle was prepared from skinned fibers by mincing with a scalpel.

Solutions

The basic rigor solution consisted of: 120 mM KCl, 5 mM $MgCl_2$, 1 mM EGTA, 40 mM MOPS, pH 7.0. In some experiments the KCl was omitted to promote tighter binding between actin and myosin, ''low-ionic-strength rigor''. In a few experiments binding was also promoted by addition of 5% (w/v) polyethylene glycol (4000 Da) to the above buffers. Experiments performed in the presence of phosphate analogs were done in the above buffer with 10 mM NaF and either 2 mM $AlCl_3$ or 2 mM $BeCl_2$ producing ~2 mM of the fluoride complexes of the two metals.

Labeling of proteins and fibers

Myosin (40 μM) was incubated with 10–80 μM of SL-ATP in the basic rigor buffer, inserted into a 50-μl capillary, and the EPR spectra was obtained. On some occasions myosin was sedimented $50,000 \times g$ for 20 min, and spectra were obtained from a pellet. Myosin subfragment S1 was exchanged into a low-ionic-strength rigor buffer, concentrated to ~350 μM using a centricon concentrator, and then labeled with 250 μM SL-ATP. The mixture was run through a spin column, and the EPR spectrum was obtained in a 50-μl capillary. The labeled S1 was then added to F-actin at a stoichiometry of ~1:3 myosin heads/actin monomers in low-ionic-strength rigor. This mixture was centrifuged at $70,000 \times g$ for 20 min. The supernatant was analyzed to determine the amount of myosin-SL-ADP remaining in solution and discarded, and the pellet containing the actomyosin complex was scraped with a spatula onto a quartz flat cell. The actin concentration in these pellets was estimated at 600 μM. The pellet was covered with a glass coverslip, sealed with vacuum grease to prevent dehydration, and placed in the cavity. Spectra of fibers were obtained from fibers that had been minced, washed twice with a rigor buffer, and labeled with a 25–50 μM solution of the appropriate SL-ATP. The fibers were then placed on the flat cell, and the excess SL-ATP was removed. Spectra of minced fibers were obtained with the cell aligned either parallel or perpendicular to the magnetic field to ensure that the sample was random.

Psoas fibers were labeled on Cys-707 with MSL following the method of Thomas and Cooke (37). In some fiber experiments, a constant flow of solution was required. Bundles of fibers ~200 μm in diameter were mounted using surgical thread into 0.5-mm diameter capillaries, placed in the cavity perpendicular to the magnetic field, and perfused with solution using a peristaltic pump.

Spin-labeled nucleotides, shown in Fig. 1, were synthesized using slightly modified procedures of previously published methods (38).

EPR spectroscopy

EPR measurements were performed with a Bruker EMX EPR spectrometer from Bruker Instruments (Billerica, MA). First derivative, X-band spectra were recorded in a high-sensitivity microwave cavity using 50-s, 100-Gauss wide magnetic field sweeps. The instrument settings were as follows: microwave power, 25 mW; time constant, 164 ms; frequency, 9.83 GHz; modulation, 1 Gauss at a frequency of 100 kHz. Each spectrum used in data analysis is an average of 5–50 sweeps from an individual experimental preparation. Measurements were done using myosin·actin pellets as follows: Temperature was controlled by blowing dry air (warm or cool) into the
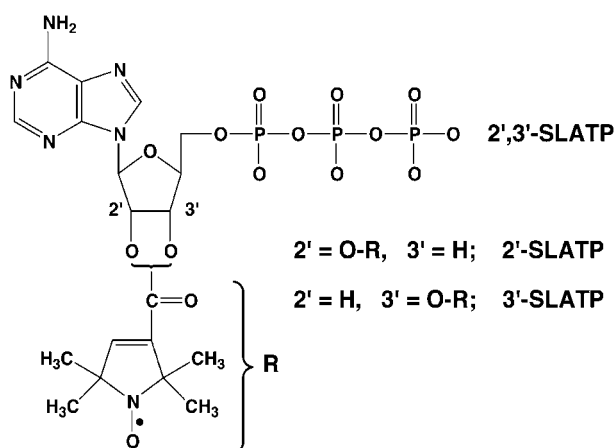
FIGURE 1   Structures of the EPR probes used in these studies. The nitroxide bond in the spin ring moiety contains an unpaired electron, denoted by a dot. In a magnetic field, the unpaired electron gives rise to a spectrum that consists of three lines, whose position and width vary with probe mobility. 2′,3′-SL-AMPPNP is identical to the 2′,3′-SL-ATP shown, except the β- and α-phosphorus atoms are linked by a nitrogen instead of an oxygen. For both 2′,3′-SL-AMPPNP and 2′,3′-SL-ATP, the label is attached to only one of the hydroxyls on the ribose but can readily isomerize between the two positions.

FIGURE 2   EPR spectra of 3′-SL-ADP bound to slow muscle myosin, in the absence (*red*) or presence (*blue*) of 2 mM AlF$_4$. The derivative of absorption is plotted as a function of the strength of the magnetic field. The width of the spectrum is 9.5 mT. The two sharp peaks P2 and P4 arise from the unbound nucleotides. The low-field and high-field peaks P1 and P5 arise solely from bound nucleotides. The greater the splitting between P1 and P5, the more immobilized is the spin probe. Both free and bound probes contribute to peak P3. Myosin, 50 μM, was mixed with 50 μM SL-ADP in rigor buffer or rigor buffer plus 1 mM AlF$_4$ and free nucleotides were removed by centrifugation before spectral acquisition. The temperature was 25°C.

cavity and monitored using a thermistor placed close to the experimental sample. We were able to control the temperature to within <2°C using this technique.

Deconvolving spectral components to obtain thermodynamic data

Spectra were deconvolved using a nonlinear least-squares method in which three basis spectra, one from bound and mobile, one from bound and immobilized, and one from unbound label, were used to determine the proportions of these components in the composite spectra seen in our samples, as described by Rice et al. (39).

Once spectra were deconvolved, the fractions of mobile and immobilized probes present in each spectrum were calculated by double-integrating component spectra to get the total amount of spin label in each component. The values for ΔG presented here are calculated by using the equation $\Delta G = -RT \ln K$, where K is the ratio of (immobilized probes)/(mobile probes). Enthalpies were calculated by creating van't Hoff plots of the data ($-R \ln K$ vs. $1/T$), using a linear least-squares fit. Entropies were calculated from the enthalpies and free energy changes using the relation $\Delta G = \Delta H - T \Delta S$.

Measurement of fiber mechanics

For mechanical experiments, single fibers were dissected from a bundle of fibers and mounted in a well between a solid-state force transducer and a rapid motor for changing fiber length as described previously (36). The ends of the fiber were fixed with glutaraldehyde to minimize end compliance, as described previously.

RESULTS

Spin-labeled nucleotides bound to myosin

The spectrum of 3′-SL-ADP bound to slow skeletal muscle myosin is shown in Fig. 2. At kinetic equilibrium, signal
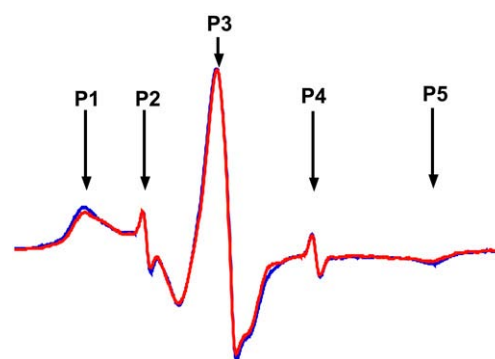
arises from both bound and unbound nucleotide. When the probe is tumbling freely in solution in times of nanoseconds or less, the spectrum consists of three narrow lines with a splitting of 1.5–1.6 mT, including peaks P2 and P4 in Fig. 2. When the probe is bound at the nucleotide site, the surface of the protein now restricts the mobility of the probe. This results in a broadening and shifting of the spectral lines, as shown by the low-field and high-field peaks, P1 and P5 in Fig. 2. Both bound and free probes contribute to peak P3. The sharp peaks corresponding to the unbound nucleotide are clearly resolved from the broader peaks at high and low field resulting from the bound nucleotide. The greater the restriction in mobility, the greater is the splitting between peaks P1 and P5, here indicating that the probe has a mobility that is moderately restricted by the protein surface. We note that the proteins in Fig. 2 are in solution, but they tumble slowly enough to be completely rigid on the EPR timescale (~200 ns). Thus, the mobility determined here shows the mobility of the probe relative to the protein rather than the tumbling of the proteins. The spectra of 2′-SL-ADP or 2′,3′-SL-ADP bound to myosin are similar to that of 3′-SL-ADP, with peaks at high and low field that indicate probes with similar but not identical mobilities (see Table 1).

The mobility observed for SL-ADP bound to myosin is determined by the degree to which the protein restricts the rotational diffusion of the nitroxide spin label. Griffith and Jost have modeled the EPR spectra of nitroxide spin probes that are undergoing rapid rotational diffusion within a cone (40). The spin probes observed here are undergoing rapid rotational diffusion restricted by the protein surface, although the region of diffusion is very likely not a geometrical cone. Nonetheless, it is constructive to compare the spectra observed here with the simulations of Griffith and Jost to

TABLE 1   Splitting between peaks P1 and P5 for the major spectral component

Proteins	Nucleotide	2′-SL-ADP	3′-SL-ADP	2′,3′-SL-ADP/2′,3′-SL-AMPPNP
F-myosin	ADP	6.4 (60)	6.5 (56)	6.5 (56)
F-myosin	ADP-AlF$_4$	6.4 (60)	6.7 (46)	6.4 (60)
F-myosin	ADP-BeF$_3$	6.4 (60)	6.6 (54)	6.4 (60)
F-myosin	AMP PNP	–	–	6.4 (60)
F-fibers	ADP	5.0 (111)*	5.4 (99)*	6.4 (60)
F-fibers	ADP-AlF$_4$	6.6 (54)	6.7 (46)	
F-fibers	ADP-BeF$_3$	6.6 (54)	6.4 (60)	
S-fibers	ADP	5.2 (105)*	5.6 (92)*	5.5 (95)
S-fibers	AMP PNP	–	–	6.5 (56)

Summary of the EPR spectral data. Column 1, proteins used: F-myosin, fast muscle myosin; F-mibers, minced fast muscle; S-mibers, minced slow muscle. Column 2, spin-labeled nucleotide and phosphate analogs used. Columns 3–5 give the P1–P5 splitting, in mT, of the dominant spectral component of the bound nucleotide in the absence and presence of actin at 25°C. The angle of the cone defining probe mobility is given in parentheses after the splitting. Peaks are defined in Fig. 2. The errors for the splittings were ~0.05 mT.

*Samples in which there is a significant second spectral component that varies with temperature.

obtain more quantitative information concerning the degree of mobility of the probes. The observed splitting between P1 and P5 in Fig. 2 suggests that the nitroxide probe of 3′-SL-ADP bound to myosin is tumbling rapidly in a region that can be approximated by a cone of full angle ~56°. The cone angle for 2′-SL-ADP bound to myosin is ~60°, which shows a lesser degree of motional restriction. The x-ray structures of myosin with a closed phosphate tube show the 3′-hydroxyl to be closer than the 2′-hydroxyl to the part of switch 1 that closed the phosphate tube. This may explain the greater steric hindrance of 3′-probe mobility. The cone angle for 2′,3′-SL-ADP is also ~55°. The cone angles are given in Table 1, in parentheses after the observed splitting.

The spectra of SL-ADP bound to fast muscle myosin in the presence of the phosphate analogs BeF$_3$ or AlF$_4$ are very similar to that of SL-ADP bound to myosin (see Fig. 2 and Table 1). The ATP analog AMPPNP binds tightly to myosin and is not hydrolyzed. Spin-labeled AMPPNP was synthesized by the same methods used for the other analogs, starting with AMPPNP. Thus, the label is attached to either the 2′- or the 3′-position. The spectrum of 2′,3′-SL-AMPPNP bound to myosin from either slow or fast muscle was very similar to that of 2′,3′-SL-ADP bound to myosin (see Fig. 3 and Table 1).

We conclude that the conformation of the nucleotide pocket of myosin restricts the rotational mobility of the attached probes within a cone with vertex angle of ~55°–60°. The spectra observed for 2′-SL-ADP, 3′-SL-ADP, and 2′,3′-SL-ADP bound to slow muscle myosin were similar to those for the species bound to fast muscle myosin. To fix notation, we term these states the ''closed conformation''. Here, ''closed'' refers to the conformation of the pocket as sensed by the spin probes, probably because of a change in the switch
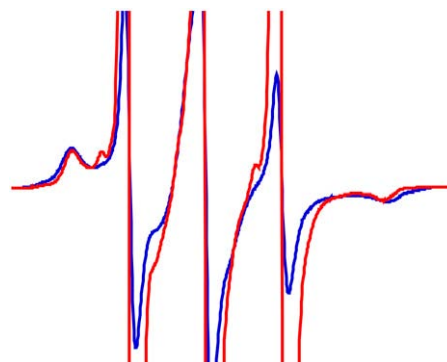

FIGURE 3   Spectrum of 2′,3′-SL-AMPPNP, an analog of ATP, bound to slow muscle myosin (*blue*) and to slow muscle actomyosin in minced fibers (*red*). The shape and position of the peaks at low and high field that arise from the bound analog change very little upon binding of the myosin to actin. This shows that the nucleotide pocket remains in the closed conformation. Spectra were obtained in rigor buffer, myosin, and in low ionic strength rigor buffer, minced fibers. Temperature was 25°C. The width of the spectrum is 9.5 mT.

1 region. The probes are not sensitive to changes in switch 2. In the Discussion, we argue that this is the same conformation as seen for crystal structures of myosin nucleotide complexes with a closed phosphate tube. However, in these spectra there is an additional minor component with higher mobility that we discuss in more detail below where we consider the temperature dependence of the spectra.

The myosin nucleotide pocket remains closed when myosin binds weakly to actin

Myosin is known to bind to actin in prepower stroke states, in which the affinity for actin is lower than observed for the rigor complex or rigor-ADP complexes that occur near the end of the power stroke (1–6). These states are transients, and to study them with EPR, they must be mimicked using nucleotide and phosphate analogs. The nonhydrolyzable analog AMPPNP produces a large decrease in the affinity of myosin for actin (41). This affinity is intermediate between the strongly binding states at the end of the power stroke and the weakly binding states at the beginning of the power stroke. As discussed above, the spectrum of 2′,3′-SL-AMPPNP bound to myosin is similar to that of 2′,3′-SL-ADP. The spectrum of 2′,3′-SL-AMPPNP bound to actomyosin in minced fibers, shown in Fig. 3, is identical within experimental error to that of the analog bound to myosin alone. A similar result is observed for both fast and slow minced fibers. Slow fibers were used in addition to fast fibers because they bind AMPPNP more tightly and because they provided a better control, discussed below. The spectra were identical in the presence and absence of 5% PEG-4000. Lowering the temperature to 5°C caused a slight broadening of the peaks, with no other changes in the spectrum. Thus, the nucleotide pocket of myosin does not change conformation on the binding of Myosin·SL-AMPPNP to actin. This is

in contrast to the result obtained for 2',3'-SL-ADP, binding to slow muscle minced fibers as described in a section below.

Several analogs of phosphate have been shown to bind with high affinity to the nucleotide site of myosin and have been studied extensively. X-ray structures have suggested that Myosin·ADP·BeF$_3$ produces an analog of the Myosin·ATP state and that Myosin·ADP·AlF$_4$ is an analog of the hydrolysis transition state intermediate (42). These analogs induce a large decrease in the affinity of myosin for actin that is similar to that resulting from the binding of ATP or ADP·Pi (43–45). As described above, the spectra of SL-ADP·BeF$_3$/AlF$_4$ bound to myosin alone are similar to those of the Myosin·SL-ADP species, indicating that the conformation of the nucleotide pocket is in a closed conformation. Because efficient binding of the phosphate analogs requires active cross-bridges, spectra were obtained from fibers in which SL-ATP was replenished by flow. The spectra of spin-labeled nucleotides show that the probes remain largely in the immobilized state on binding to actin in either the Actin·Myosin·ADP·BeF$_3$ or Actin·Myosin·ADP·AlF$_4$ states (see Fig. 4 and Table 1). The spectrum obtained in the presence of these phosphate analogs is highly disordered; thus, the spectra obtained from the oriented fibers was independent of the orientation of the fibers relative to the magnetic field and report only probe mobility. These results, along with those obtained using 2',3'-SL-AMPPNP, imply that the nucleotide pocket remains closed in the more weakly bound states near the beginning of the power stroke. The opening of the nucleotide pocket observed for the diphosphate analogs, described below, requires the strong bond with actin, which is found near the end of the power stroke.

Is the myosin head bound to actin in the weakly bound states?

The conclusions drawn above regarding the weakly binding actomyosin states require that a substantial fraction of the
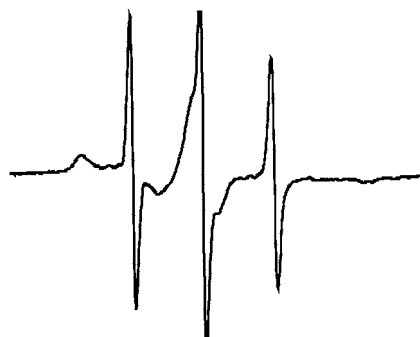

FIGURE 4 EPR spectrum of 2'-SL-ADP·AlF$_4$ bound to myosin in fast muscle fibers, showing that there is no observable opening of the nucleotide pocket, as measured by probe mobility. Spectra were obtained during constant flow with a low ionic strength rigor solution containing 5% PEG-4000 at 25°C, conditions that promote binding of myosin to actin. The width of the spectrum is 9.3 mT.

myosin in the minced fibers be in fact bound to actin in the presence of the nucleotide and phosphate analogs used to mimic the weakly bound states. To ensure that a large fraction of myosin was bound to actin during spectral acquisition, we used conditions that promote the formation of the bond with actin. These were higher temperatures, 25°C, lower ionic strength, and the addition of a polymer, PEG-4000, that potentiates protein-protein interactions, including the binding of myosin to actin (46).

In the presence of AMPPNP, binding to actin was assessed by two methods. We determined whether the catalytic domain of myosin was oriented with respect to the fiber axis, and we measured fiber stiffness. Previous work has shown that probes bound to the myosin catalytic domain in muscle fibers at Cys-707 are randomly oriented when myosin is not bound to actin and are highly oriented when myosin is bound to actin (37). The spectrum of Cys-707-labeled fibers, shown in Fig. 5, displays these two components, labeled random and ordered. Our control results again show that Cys-707-labeled fibers are oriented in the rigor state (Fig. 5 A) and disordered in the relaxed state (Fig. 5 D). The catalytic domain remains oriented as in rigor in the presence of 5 mM MgAMPPNP (Fig. 5 B), consistent with previous observations of Fajer and co-workers (47). This indicates that >90% of the Myosin·AMPPNP complexes are bound to actin under these conditions. As an additional control, spectra were accumulated in a high-ionic-strength buffer additionally containing 37% glycerol. These conditions have been previously shown to reduce the affinity of the Myosin·AMPPNP complex to actin in fibers while not affecting the affinity of the rigor complex (48). As seen in Fig. 5 C, the spectrum becomes disordered, showing that the myosin heads are dissociated from actin by the binding of AMPPNP under these conditions.

Fiber stiffness was also used to monitor actomyosin bond formation. Stiffness is low when myosin is detached from actin and is high when myosin is attached. The stiffness of slow twitch fibers in the presence of AMPPNP is 98 ± 4% (mean ± SE, $n = 30$) of that in rigor, where all myosin heads are bound to actin in low-ionic-strength rigor at 25°C. Similar results were obtained in fast muscle fibers. The affinity of AMPPNP for fast muscle Actin·Myosin has been determined to be 2×10^2 M^{-1} (47,49). With this affinity ~44% of the actin-myosin complexes are bound to AMPPNP. The affinity of nucleotides for slow muscle Actin·Myosin is greater than for fast. The affinity of SL-AMPPNP for Actin·Myosin in the fibers can be determined from the spectrum of Fig. 3, which shows that ~55% of the SL-AMPPNP is bound to myosin, indicating an affinity constant of $8 \pm 2 \times 10^3$ M^{-1}. This affinity shows that at the concentrations employed in the measurements of fiber stiffness, 5 mM, in slow fibers ~97% of myosin heads are bound to AMPPNP. Thus, the lack of change in the orientation of probes on Cys-707 or in fiber stiffness shows that the majority of myosin-AMPPNP heads, >90%, are bound to actin. Together the orientation of the
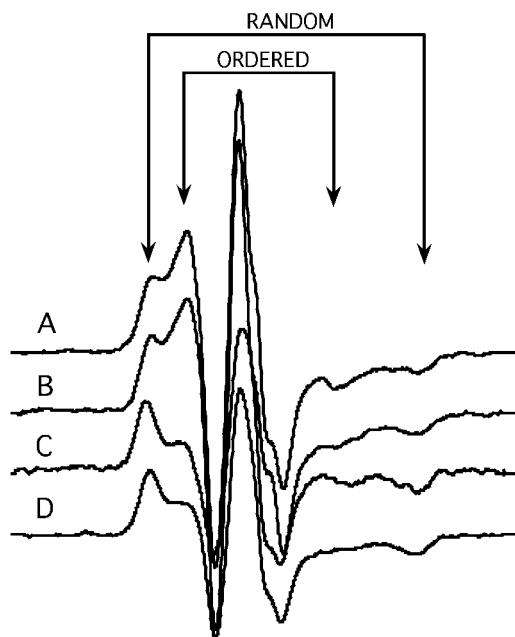
FIGURE 5 EPR spectra of maleimide spin probes attached to Cys-707 on the myosin catalytic domain in fast muscle fibers were used to measure the orientation of this domain. The spectra consist of two components, one in which the orientation of the probes is ordered by the bond between myosin and actin and one in which the myosin is detached from actin, and the orientation of the catalytic domain is random. The high- and low-field peaks of each component are labeled. The top spectrum (A) shows heads oriented in rigor, 25°C, and the bottom spectrum (D) shows heads that are disordered in relaxed fibers, 25°C. In the presence of 4 mM AMPPNP (25°C, low ionic strength) the heads remain oriented, showing they are bound to actin (B). Changing conditions to 4 mM AMPPNP, 37% glycerol, and high ionic strength (0.22 M) releases the heads from actin (C). The width of the spectrum is 12.5 mT.

catalytic domain and the high fiber stiffness show that AMPPNP causes no detectable dissociation of myosin from actin under these conditions; thus, the spectra of Fig. 3 show that the conformation of the myosin nucleotide pocket remains closed in the ternary Actin·Myosin·SL-AMPPNP complex for both fast and slow myosin.

The fraction of myosin heads bound to actin in the presence of the phosphate analogs was determined by measuring stiffness only, as the orientation of the catalytic domain of myosin is disordered in the presence of the phosphate analogs, and thus orientation cannot be used to evaluate formation of the actomyosin bond (50). The phosphate analogs bind to myosin very strongly, even in the presence of actin, and the isometric force exerted by the fibers in the presence of the concentrations used was <5% of control. Thus, virtually all myosin heads are bound to the phosphate analogs, but are these heads also bound to actin? In the conditions used to obtain spectra in the presence of the phosphate analogs, low-ionic-strength rigor, 25°C, 5% PEG-4000, the affinity of the weak states for actin is potentiated. Fiber stiffness under these conditions has been shown to be high, ~60% of rigor in the presence of a similar phosphate analog,

vanadate (46). We found a similar result for the analogs employed here with stiffness of 55 ± 10% of rigor for active slow or fast muscle fibers inhibited in the presence of either BeF_3 or AlF_4. Stiffness is not a simple measure of the fraction of myosin heads attached to actin because the cross-bridge compliance is in series with the compliance of the filaments as well as compliance external to the sarcomere, e.g., at attachment points of the fiber to the apparatus. If we assume that the cross-bridge compliance is only one third of the total compliance, the observed change in stiffness of 40% suggests that ~20% of the myosin heads remain attached to actin in the presence of the analogs. There were no discernable probes in the more mobile state in the spectra obtained with any of the phosphate analogs (e.g., see Fig. 4). We conclude that the probes attached to bound nucleotides remain in the immobilized state in the presence of either analog and that the nucleotide pocket of Actin·Myosin remains predominantly in the closed conformation.

The nucleotide pocket is more open in the strongly bound Actin·Myosin·SL-ADP states

Fig. 6 shows the spectra obtained from 2′-SL-ADP bound to fast muscle myosin and to actomyosin in minced fibers. Minced fibers were used because the high concentrations of myosin and actin provided a large ratio of bound to free nucleotide and also ensured that all the myosin was bound to actin. Similar spectra were obtained for fibers and actoS1 (see Fig. 6). As can be seen, a new component is present in the actin-bound spectrum with an observed splitting of 5.0–5.6 mT. This corresponds to rotational mobility of the probe being restricted to a cone of ~90–110°. We call this protein conformation the ''open conformation''. Here ''open'' refers to the conformation of the pocket sensed by the spin probes, probably because of a change in the switch 1 region. The probes are not sensitive to changes in switch 2. As is also evident from Fig. 6, there is a second spectral component similar to that observed for the closed state, indicating an equilibrium between the open and closed conformations of myosin. There is also a small component of the open state in the spectrum of myosin or S1 alone.

The spectrum of the SL-ADP species bound to minced fibers depended on both the nucleotide analog and the isoform of myosin used. In all cases, similar open and closed conformations were seen; however, the relative proportions of the two states varied. With both fast and slow muscle, the spectra of 2′-SL-ADP and 3′-SL-ADP were similar, showing a higher fraction of the open conformation at 25°C. However, the spectral intensities from 2′,3′-SL-ADP bound to fast muscle showed that the nucleotide pocket was mostly in the closed conformation at 25°C, whereas in the slow muscle, it was in the open conformation (see Table 1). The difference between these analogs is that in the 2′,3′-SL-ADP, the label is attached to either the 2′- or the 3′-position, with an easy isomerization between the two positions,
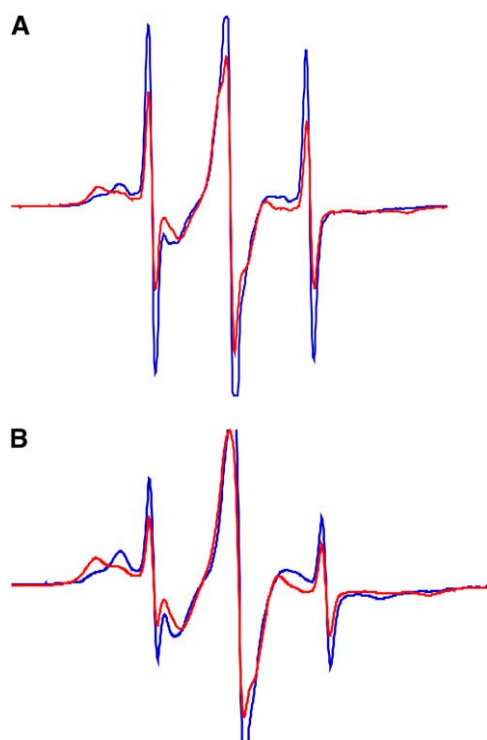
FIGURE 6 (*A*) EPR spectra of 2′-SL-ADP bound to fast muscle myosin (*red*) and to fast Actin·Myosin in fibers (*blue*). The shift in the splitting between the two spectra shows that the probe becomes more mobile (nucleotide pocket more open) when myosin binds to actin. The Actin·Myosin spectrum was obtained from a pellet of minced fibers in rigor buffer. (*B*) The EPR spectrum of 2′-SL-ADP bound to S1 (*red*) and to actoS1 (*blue*). The spectra were obtained in low-ionic-strength rigor buffer at 25°C. The width of the spectrum is 9.0 mT.

leaving a hydroxyl on the unoccupied position (see Fig. 1). With 2′-SL-ADP and 3′-SL-ADP, the ribose position not occupied by the label is occupied by a hydrogen atom bound to the ring carbon. Thus, slow fibers provide a better comparison with the spectra of 2′,3′-SL-AMPPNP, showing that the nucleotide pocket is closed in 2′,3′-SL-AMPPNP and open in 2′,3′-SL-ADP. In the case of fast fibers, the nucleotide pocket is closed in both cases. The differences between fast and slow fibers are currently under further investigation and will be described in a subsequent article.

The temperature dependence of the spectra defines the thermodynamics of the transition between open and closed conformations

As discussed above, the spectra of Actin·Myosin·SL-ADP display two components corresponding to the open and closed states. The relative magnitudes of the two components were temperature dependent, with the closed state favored at lower temperatures. The spectrum of Actin·S1·2′-SL-ADP is predominantly closed at 2°C and predominantly open at 30°C. This suggests that the two conformations of the

nucleotide pocket are in equilibrium when Myosin·SL-ADP is bound to actin. To better define the thermodynamics of this open-to-closed transition, the spectra of the complex of fast Myosin S1·2′-SL-ADP in complex with actin were obtained as a function of temperature and deconvolved into their two bound components to obtain the populations of the two states, as described in Methods and shown in Fig. 7. Approximately pure spectral components were obtained for the mobile and immobile bound probes and used to deconvolute the spectra obtained at different temperatures (see Fig. 7 *A*). Double integration of the spectral components defined the populations of each, which were used to determine an equilibrium constant, $K = $ [immobile fraction]/[mobile fraction]. The equilibrium constant between the two conformations was determined as a function of temperature. Fig. 7 *B* shows a plot of $-R\ln(K)$ vs. $1/T$ from these fits. Using the van't Hoff relationship, the slope of a least-squares linear fit to the data over the temperature range 8–29°C yields a $\Delta H^0 = -79 \pm 5$ kJ/mol, $\Delta S = -0.28 \pm 0.02$ kJ/mol K. These large values for ΔH^0 and ΔS imply a significant conformational change at the myosin nucleotide site. However, the conformational change involves a relatively low free energy difference, with equal populations at 283 K and with the open conformation favored at higher temperatures.

The spectra of the SL-ADP species bound to myosin alone were composed mainly of a single component, indicating a moderately immobilized probe. However, Fig. 6 shows there was also a small component associated with the more mobile probe. The change in the spectrum with temperature, however, was not great, suggesting that for Myosin·SL-ADP, the closed conformation of the nucleotide pocket is greatly favored. In the presence of the phosphate analogs AlF_4 and BeF_3, the nucleotide pocket was entirely in the closed conformation at all temperatures, indicating that the free energy favoring the closed conformation is even greater.

DISCUSSION

Interpretation of the EPR spectra

Spin-labeled nucleotides provide a highly effective reporter group for monitoring the conformation of the nucleotide-binding site of myosin. In these analogs, the spin probe is connected to the nucleotide ribose via a short linker (Fig. 1). This places the spin probe directly in the active site, positioning it in an excellent position to be perturbed by conformational changes in the adjacent protein surface (see Fig. 8). In the presence of 1 mM ATP, which competes with the binding of the spin-labeled nucleotides, the signal from the bound nucleotides is lost entirely, showing the high specificity of the SL-ADP for the active site. Similar spin-labeled nucleotides have previously been found to provide a sensitive method for monitoring the active site of two kinesin-family motors, which have active site conformations that have substantial similarity to those of myosin (15).
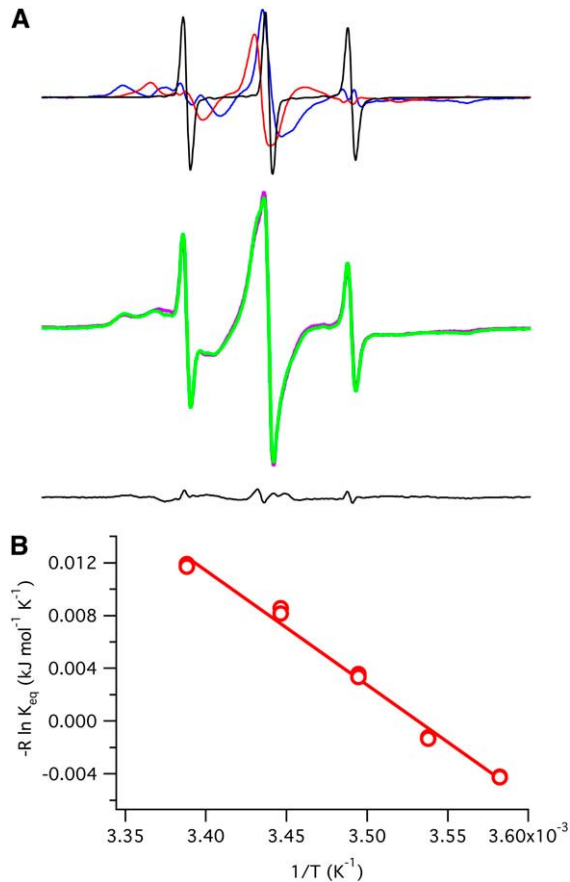
FIGURE 7 Deconvolution of spectra and van't Hoff plot. (*A*) The fitting procedure to determine the relative contribution of the more immobilized and more mobile components in the EPR spectra from 2′-SL-ADP as a function of temperature is shown. Top spectra, spectral components associated with open and closed nucleotide pockets (*red* and *blue*, respectively); free probe (*black*). Middle spectra, Actin·fast-S1·2′-SL-ADP at 9.5°C (*purple*), fit to the spectrum (*green*). Bottom spectrum, difference spectrum between experimental data and fit. (*B*) Spectra of Actin, fast muscle S1 and 2′-SL-ADP were obtained as a function of temperature and deconvolved. The populations associated with the two components were used to calculate an equilibrium constant, which was used to determine a van't Hoff plot, shown. The van't Hoff plot yielded a $\Delta H = -79 \pm 5$ kJ/mol, $\Delta S = -0.28 \pm 0.02$ kJ/mol K.

The high-field to low-field splitting from spectra of myosin bound to SL-ADP or the analogs SL-AMPPNP, SL-ADP·BeF$_3$, or SL-ADP·AlF$_4$ all show probes that are moderately immobilized by the adjacent protein surface, effective cone vertex angles of ~55–60°. Similar spectra are observed for both fast and slow skeletal myosin. There is a slight though somewhat variable trend for the triphosphate-analog states to be more immobilized. The analog SL-ADP·BeF$_3$ is probably a mimic of the ATP states (42). The analog SL-AMPPNP may also resemble a triphosphate state, but the affinity for actin is much greater than that observed for ATP. There is no difference in the EPR spectra between these states and states that mimic the hydrolysis transition state intermediate, e.g., SL-ADP·AlF$_4$. There was little

temperature difference in the results. We consider all these states as the closed state, and below we suggest that it corresponds to the nucleotide closed states seen in crystal structures of myosin (7).

With the Actin·Myosin·SL-ADP species, a major new spectral component was observed corresponding to EPR probes that were significantly more mobile than observed for myosin species alone. The effective modeled vertex cone angle of mobility increased to 90°–110° for these species. We interpret this to indicate an opening of the nucleotide pocket in the ADP states in the presence of actin, which is not present in the triphosphate states. This more mobile component was similar in both fast and slow skeletal muscle. We term this component the open state. In a section below we suggest that the open conformation is the result of a movement of the switch 1 region, as shown in some crystal structures and EM reconstructions.

The probes attached to analogs of states with a phosphate in the γ-position, either with AMPPNP or the phosphate analogs, remained as immobilized as in the absence of actin. Although control experiments showed that appreciable fractions of myosin heads in these states were bound to actin, the more mobile component seen with strongly bound Actin·Myosin·SL-ADP was never observed. We conclude that the myosin nucleotide pocket remains closed in the more weakly bound states at the beginning of the power stroke.

Energetics of the closed-to-open transition of the nucleotide pocket

A real strength of EPR spectroscopy over other spectroscopic and crystallographic techniques is its ability to resolve multiple conformations of the proteins under conditions modeling the physiological conditions of functioning muscle. Our Actin·Myosin·SL-ADP spectra show two distinct spectral components. One corresponds to the closed conformation seen in the absence of actin and in the actin-bound triphosphate-analog states; the other is the open conformation.

In the Actin·Myosin·SL-ADP states, the relative fractions of myosin in the open and closed states were temperature dependent. The van't Hoff plot shown in Fig. 7 defines the thermodynamic parameters. The changes in enthalpy and entropy between the two conformations indicate that a significant number of amino acids are involved in the conformational change. However, the free energy difference between the two conformations is relatively modest, only ~1.5 $k_\mathrm{B}T$ at 20°C. The equilibrium between the open and closed conformations of the nucleotide pocket in the Actin·Myosin·SL-ADP complexes appears to be influenced by the structure of the spin-labeled nucleotide. The observation that the closed conformation is more favored in the 2′,3′-SL-ADP enantiomer species than in the deoxy-analogs, 2′-SL-ADP and 3′-SL-ADP, suggests that the presence of the hydroxyl on the position unoccupied by the label influences the equilibrium. The spin label can isomerize between the 2′- and
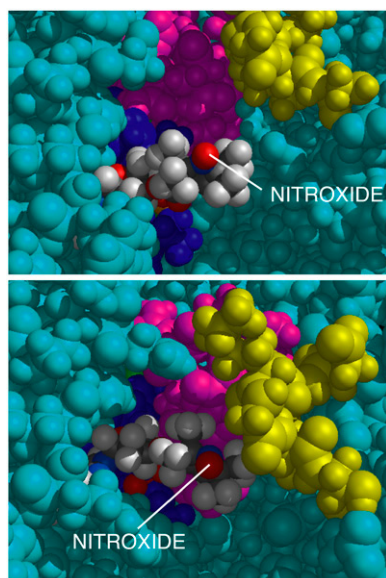
FIGURE 8   To understand better the structural basis of the EPR spectra, the structure of 2′-SL-ADP was docked into the structure of Reubold et al. (19), which shows a very open nucleotide-binding site (*above*), and into the *Dictyostelium* myosin·ADP·BeF$_3$ structure, which has a closed nucleotide site (*below*) (42). Three structures are identified: the P-loop (*blue*); switch 1 (*magenta*); and amino acids 314–319 (*yellow*). 2′-SL-ADP was docked (via a P-loop superposition with the myosin·ADP·BeF$_3$ structure) into the nucleotide-free myosin structure of Reubold et al. (19). The molecules are shown as CPK surfaces. In this closed structure, it is clear that there is significant steric interference affecting probe mobility from the switch 1 region and from the adjacent loop, amino acids 314–319. The closed structure would appear to be compatible with the degree of mobility we observe for the immobile EPR spectra, The magnitude of the displacement of switch 1 and amino acids 314–319 in the Reubold structure results in a very open nucleotide pocket, which appears too open to be compatible with our EPR spectra. However, further molecular dynamics simulations will be required to establish whether the spectra are compatible with either structure.

3′-hydroxyls in this compound, and we do not know which position is favored in the bound analog. The fact that both ribose hydroxyls can form hydrogen bonds whereas the deoxy ribose hydrogen cannot may offer an explanation for the differences. However, myosin x-ray structures show little interaction of the 2′- or 3′-hydroxyls of the ribose with the protein. It is possible that interactions between protein and nucleotide not visualized in the crystal structures play a role in the interaction. We also observe that, in the actin-free Myosin·2′-SL-ADP and Myosin·3′-SL-ADP complexes, the closed conformation is also in equilibrium with the open conformation, but the fraction in the open conformation is very small (see Fig. 2), and the temperature dependence is very weak. Addition of phosphate analogs eliminated this more mobile component for both myosin and Actin·Myosin at all temperatures. These data show that the closed conformation is strongly favored in myosin alone, and it is even more favored in the presence of a phosphate analog bound at the γ-phosphate position.

Our observations lead to a model of the conformational changes occurring in the nucleotide pocket of myosin shown in Fig. 9. The myosin nucleotide pocket is closed when detached from actin. It remains closed when it initially attaches to actin with ATP or ADP·Pi at the nucleotide site. The nucleotide pocket then opens in the strongly bound Actin·Myosin·ADP state and presumably in the strongly bound rigor state as well, although we cannot observe this state with our nucleotide probes. The transition from the closed to the open conformation occurs at some point after the release of phosphate and before the release of ADP near the end of the working stroke in state 4, however the exact point at which it occurs is not certain.

Docking of the nucleotide analog spin probes into myosin x-ray structures

To better understand the structural basis of the changes in EPR spectra, the structure of 2′-SL-ADP was docked into the closed phosphate-tube nucleotide-binding site of the *Dictyostelium* Myosin·ADP·BeF$_3$ structure (42) using the ADP in the x-ray structure as a template for positioning the analog. This structure was then superimposed via a least-squares P-loop distance minimization on the open nucleotide pocket structure of Reubold et al. (19), and 2′-SL-ADP was then directly annealed into the open structure, generating an open phosphate-tube structure. Results are shown in Fig. 8. Examination of the closed phosphate-tube structure showed that there was significant steric interference with probe mobility from the switch 1 region (*magenta*) and from an adjacent loop, amino acids 314–319 (*yellow*). Additionally, the docking suggests that a 2′-probe would experience less steric hinderance than a 3′-probe because of its ~1.5 Å increased distance from switch 1 and amino acids 314–319. The data in Table 1 are consistent with this observation. Thus, the *Dictyostelium* structure (42) would appear to be compatible with the degree of mobility we observe for the immobile EPR spectra. In some preliminary investigations, the mobility of the docked 2′-probe was determined by molecular dynamics in a calculation similar to that performed for spin probes attached to nucleotides bound to microtubule motors (15). The goal of these calculations is to establish a more quantitative connection between probe mobility and protein structures. These calculations suggest that the observed mobility was consistent with the structure of myosin with a closed nucleotide pocket. However, further molecular dynamics simulations will be required to establish this.

There is structural homology between the nucleotide site of kinesin-family motors and myosin. We have previously used EPR spectroscopy to demonstrate a closing of the nucleotide site of kinesin motors (15). When compared to myosin structures, kinesin-family x-ray structures show an open phosphate tube as a result of displacement of switch 1 away from the nucleotide site. We have demonstrated that the spectroscopic results can be explained by a closing of the
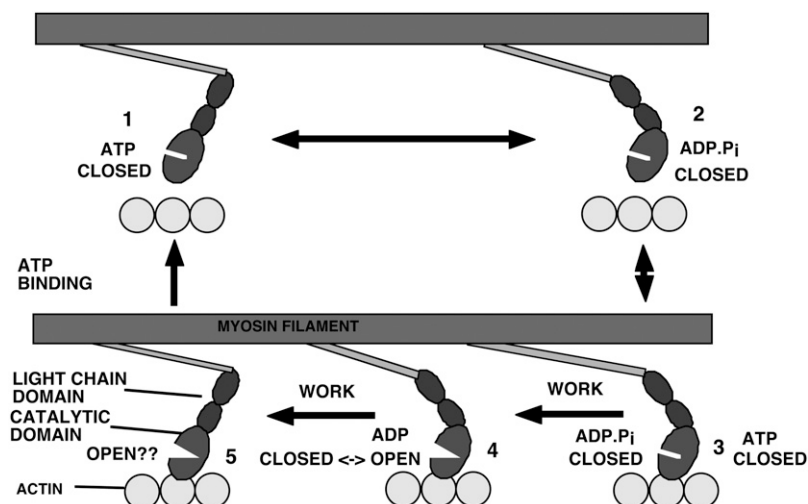
FIGURE 9 A schematic of the actomyosin cycle, showing the conformation of the nucleotide site as deduced from our work. Force is generated by states 4 and 5 and by some substates within state 3. The nucleotide site is in the closed conformation when myosin is not bound to actin (states *1* and *2*). It remains closed when myosin binds to actin with either ATP or ADP-Pi bound to the active site (state *3*). In the strongly bound Actin-Myosin-ADP state it has an open conformation (state *4*). The exact point at which the transition occurs between open and closed may occur within state 4 and not in the transition between states 3 and 4, as discussed in the text.

phosphate tube via a displacement of switch 1 into the position seen in myosin structures with a closed phosphate tube, e.g., the *Dictyostelium* Myosin·ADP·BeF$_3$ structure (14,15). The EPR probes appear to be more mobile in the closed kinesin-family motors. The docking in Fig. 8 again suggests that this is to be expected. The structure formed by amino acids 314–319 is not present in kinesin-family motors, so less steric hinderance would be expected.

In the open crystal structures, the opening of the nucleotide pocket results from a bending of the core β-sheet platform of myosin (19). The bending of the β-sheet results in a significant displacement ($\sim$5 Å) of switch 1 and the structure formed by amino acids 314–319 away from the bound nucleotide (Fig. 8 *A*). The magnitude of this displacement results in a very open nucleotide pocket in the myosin II x-ray structure. Both of these open structures have been proposed to represent the actin-bound conformation of myosin. However, our preliminary docking of 2′-SL-ADP into the open structure suggests that these structures would result in an observed EPR probe mobility that is significantly larger than even the most mobile EPR spectra in Table 1. The EPR probes appear to be seeing an actin-bound state different from that proposed on the basis of x-ray crystallography; however, molecular dynamics simulations will be required to make a more definitive conclusion.

Relationship to other studies

We originally proposed an opening of the nucleotide site of myosin on the basis of the observation that nucleotide analogs with moieties attached to the γ-phosphate position, which were too large to fit through the closed phosphate tube, still bound to myosin and to actomyosin (11). Here we have extended these studies by placing a spectroscopic reporter group directly in the active site to monitor an opening and closing of the nucleotide site. Several other spectroscopic methods have been used to probe changes in myosin

on binding and hydrolysis of nucleotides. Bagshaw and co-workers constructed myosin catalytic domains from *Dictyostelium* myosin II with only one tryptophan (26,51). Tryptophans in the β-sheet at the N-terminus of switch 1 at the nucleotide site (F239W and F242W) showed a blue shift and decrease in fluorescence on binding and hydrolysis of nucleotides. The decrease associated with W239 was enhanced by the binding of actin. Berger and co-workers engineered a single tryptophan into the upper 50-kDa domain of smooth muscle myosin motor domain (F344W) and observed a change in FRET signal between W344 and MANT-nucleotides at the nucleotide site (29). These corresponded to distances of 29 Å and 33 Å in the triphosphate and diphosphate states, respectively. Yengo and co-workers measured a FRET signal between MANT-nucleotides and a biarsenical compound attached to the upper 50-kDa domain in myosin V and found a similar increase in distance between tri- and diphosphate nucleotide states (30). These were interpreted in terms of opening of switch 1 occurring on phosphate release. The results obtained here with skeletal myosin show only modest changes between SL-ADP analogs and analogs that simulate the Myosin·triphosphate states, and the difference between our conclusions and those of these two previous investigations may be the result of isoform differences. Preliminary EPR spectroscopy shows larger differences between tri- and diphosphate states for smooth muscle myosin (52). Thus, there is now general agreement in the above studies that the conformation of the nucleotide site of myosin changes in response to the state of the nucleotide and that it is more open in Myosin·ADP than in Myosin·ADP·Pi or Myosin·ATP.

Results from a variety of techniques now agree that the nucleotide site of myosin adopts a more open conformation on binding to actin. Modeling of cryoelectron microscopy reconstructions of the actomyosin complex led to the conclusion that a rotation of the upper 50-kDa domain and opening of the nucleotide pocket was associated with the binding of

myosin to actin (21,23). Crystal structures of a chimera of the *Dictyostelium* myosin II motor domain and the GTPase domain of dynamin (19) and of myosin V (17,18) and myosin VI (20) all provided further evidence for a rotation of the upper 50-kDa domain and a concurrent opening of the nucleotide pocket via a shift in the position of the switch 1 region away from the bound nucleotide (17,18). These open x-ray structures have been postulated to be actin-bound states, although actin was not present in any of the x-ray structures. X-ray structures have also suggested that there are conformational changes in the switch 2 region that are associated with the working power stroke. However, the x-ray structures also suggest that these occur in a region of the protein that is not expected to influence the mobility of probes attached to the ribose of bound nucleotides. We previously showed that analogs with large moieties attached to the γ-phosphate could bind to myosin or to actomyosin. A further analysis of those data demonstrated that these analogs bound 3–15 times more easily to the actomyosin complex than to myosin, also supporting the opening of the nucleotide pocket in the actomyosin complex. Our present data show that in myosin alone there is a small fraction of nucleotide pockets in the open conformation, which would explain the ability of these analogs to bind to myosin. Thus, these previous results, along with the current observations of spin probe mobility, agree that the nucleotide pocket of myosin opens on binding to actin. However, not all probes of the nucleotide site have reported a more open conformation, and ATP with a spin probe attached to both the 2′- and 3′-hydroxyls shows less mobility when the myosin binds actin, The difference between these results and those reported here and by others could arise because both positions on the ribose are blocked (32).

The spectra of bound spin-labeled nucleotides show that the myosin nucleotide site remains closed in the weakly bound prepower-stroke states, Actin·Myosin·ATP and Actin·Myosin·ADP·Pi. The distance between MANT-nucleotides and a flurophore in the upper 50-kDa domain of myosin V also showed no change on binding to actin in these states (30). However, this distance also did not change on release of phosphate to form Actin·Myosin·ADP, suggesting that myosin V may be different from myosin II in the actin bound states.

A major conclusion of the current work is that the conformation of the nucleotide is in an equilibrium between open and closed conformations in the Actin·Myosin·ADP state. In both of these states, the bond between actin and myosin is strong. Multiple states for Actin·Myosin·ADP have been previously identified in smooth muscle acto·S1 using a fluorescent nucleotide (28). In two of these states, myosin is strongly bound to actin, and the affinity for ADP is either weak or strong. The state with greater affinity for ADP is favored by lower temperatures and presumably corresponds to our closed nucleotide pocket, whereas the more weakly binding state would correspond to our open nucleotide pocket. However, only one state was observed by the

fluorescent nucleotides in a myosin II from *Dictyostelium*. Two states of skeletal Actin·Myosin·ADP that differ in their tryptophane fluorescence and that have an equilibrium between them of close to unity were identified by Trybus and Taylor (53). These may correspond to the two states seen here. However, the thermodynamics of the transitions between the states identified by fluorescence have not been measured, and establishing the correspondence between them and the states identified here by EPR requires more work.

Conformation of the actin-binding cleft

Our observations are relevant to currently popular hypotheses regarding the myosin actin-binding cleft. The initial structure of chicken S1 suggested that the myosin actin-binding cleft closed on binding to actin (7). Biochemical data have coupled cleft closing to formation of the strongly bound actomyosin complex (21,22,25,31). X-ray structures of myosin II constructs and of myosin V and cryoelectron microscopy modeling have further coupled the closing of the actin-binding cleft to a concomitant opening of the nucleotide site via switch 1 movements (17,18,23). This would be reasonable if the upper 50-kDa domain moved as an approximately rigid domain because one face of this domain forms one side of the actin-binding cleft while its opposite face forms one side of the nucleotide pocket. Accepting this linkage between conformational changes in switch 1 and actin-binding cleft, our conclusion that the nucleotide pocket is in an equilibrium between open and closed conformations implies that the actin-binding cleft must also exist in an equilibrium between open and closed conformations. The more open conformation of the actin-binding cleft is favored in myosin alone, whereas the closed conformation is favored in the actomyosin complex. From the data of Fig. 7, at in vivo temperatures the closed cleft would be favored by ∼3 k_BT. Thus, the closing of the nucleotide cleft is not obligatory for formation of the strongly bound actomyosin state. Indeed, structural considerations suggest that an equilibrium between an open/closed actin-binding cleft, correlated with a closed/open nucleotide pocket, is in fact not unreasonable. Models of the actomyosin complex show an extensive interaction between the lower 50-kDa domain and actin, but the corresponding interaction of the upper 50-kDa domain with actin is more tenuous. Thus, although the rigid rigor bond is determined by the interaction of the lower 50-kDa domain, the orientation of the upper 50-kDa domain could be fluctuating between open and closed forms. Indeed, preliminary reports monitoring the conformation of the actin-binding cleft via dipole-dipole interactions between EPR probes on opposite sides of the cleft have concluded that the cleft has two conformations, one more open than the other, but that both forms are seen in both myosin and the actomyosin complex (24,27). We finally note that our results cannot rule out models in which there is not a tight coupling between the opening and closing of the nucleotide site and the actin-binding cleft.

SUMMARY

We conclude that spin-labeled nucleotides provide an effective way to monitor the conformation of the nucleotide site of myosin. The spectra show that the nucleotide pocket of myosin is predominantly in a closed conformation for myosin alone. When the labeled nucleotide bound to myosin is in a state that mimics either ATP or ADP·Pi, the pocket does not open when myosin binds weakly to actin. In the strongly bound Actin·Myosin·SL-ADP states, the energetics of the nucleotide pocket favors a more open conformation. In these states, the open and closed conformations are in equilibrium, with the open state favored by higher temperatures. An opening of the myosin nucleotide pocket by a displacement of the switch 1 region would be expected to weaken the affinity of myosin for nucleotides, thus promoting the release of ADP and phosphate. In the crystal structures of myosin V with ADP bound to an open myosin pocket, the affinity of the nucleotide is very low (18). There- fore, our results, which show that opening of the nucleotide pocket occurs only in the strongly bound states, appear rea- sonable, as this would tend to keep ADP bound until the end of the working stroke. Thus, if force is generated in the weakly bound states as suggested by some studies (36,54,55), our data show that force is initially generated by a myosin with closed nucleotide pocket.

REFERENCES

1. Cooke, R. 1997. Actomyosin interaction in striated muscle. *Physiol. Rev.* 77:671–697.

2. Holmes, K. C. 1996. Muscle proteins—their actions and interactions. *Curr. Opin. Struct. Biol.* 6:781–789.

3. Geeves, M. A. 1991. The dynamics of actin and myosin association and the crossbridge model of muscle contraction. *Biochem. J.* 274: 1–14.

4. Geeves, M. A., R. Fedorov, and D. J. Manstein. 2005. Molecular mechanism of actomyosin-based motility. *Cell. Mol. Life Sci.* 62:1462– 1477.

5. Cooke, R. 2004. The sliding filament model: 1972–2004. *J. Gen. Physiol.* 123:643–656.

6. Spudich, J. A. 1994. How molecular motors work. *Nature.* 372: 515–518.

7. Rayment, I., W. R. Rypniewski, K. Schmidt-Base, R. Smith, D. R. Tomchick, M. M. Benning, D. A. Winkelmann, G. Wesenberg, and H. M. Holden. 1993. Three-dimensional structure of myosin subfrag- ment-1: A molecular motor. *Science.* 261:50–57.

8. Kull, F. J., and S. A. Endow. 2002. Kinesin: switch I & II and the motor mechanism. *J. Cell Sci.* 115:15–23.

9. Smith, C. A., and I. Rayment. 1996. Active site comparisons highlight structural similarities between myosin and other P-loop proteins. *Biophys. J.* 70:1590–1602.

10. Vale, R. D. 1996. Switches, latches, and amplifiers: common themes of G proteins and molecular motors. *J. Cell Biol.* 135:291–302.

11. Pate, E., N. Naber, M. Matuska, K. Franks-Skiba, and R. Cooke. 1997. Opening of the myosin nucleotide triphosphate binding domain during the ATPase cycle. *Biochemistry.* 36:12155–12166.

12. Kull, F. J., R. D. Vale, and R. J. Fletterick. 1998. The case for a common ancestor: kinesin and myosin motor proteins and G proteins. *J. Muscle Res. Cell Motil.* 19:877–886.

13. Kull, F. J., E. P. Sablin, R. Lau, R. J. Fletterick, and R. D. Vale. 1996. Crystal structure of the kinesin motor domain reveals a structural similarity to myosin. *Nature.* 380:550–555.

14. Minehardt, T. J., R. Cooke, E. Pate, and P. A. Kollman. 2001. Molecular dynamics study of the energetic, mechanistic, and structural implications of a closed phosphate tube in ncd. *Biophys. J.* 80:1151– 1168.

15. Naber, N., T. J. Minehardt, S. Rice, X. Chen, J. Grammer, M. Matuska, R. D. Vale, P. A. Kollman, R. Car, R. G. Yount, R. Cooke, and E. Pate. 2003. Closing of the nucleotide pocket of kinesin-family motors upon binding to microtubules. *Science.* 300:798–801.

16. Naber, N., S. Rice, M. Matuska, R. D. Vale, R. Cooke, and E. Pate. 2003. EPR spectroscopy shows a microtubule-dependent conforma- tional change in the kinesin switch 1 domain. *Biophys. J.* 84:3190– 3196.

17. Coureux, P. D., A. L. Wells, J. Menetrey, C. M. Yengo, C. A. Morris, H. L. Sweeney, and A. Houdusse. 2003. A structural state of the myosin V motor without bound nucleotide. *Nature.* 425:419–423.

18. Coureux, P. D., H. L. Sweeney, and A. Houdusse. 2004. Three myosin V structures delineate essential features of chemo-mechanical trans- duction. *EMBO J.* 23:4527–4537.

19. Reubold, T. F., S. Eschenburg, A. Becker, F. J. Kull, and D. J. Manstein. 2003. A structural model for actin-induced nucleotide release in myosin. *Nat. Struct. Biol.* 10:826–830.

20. Menetrey, J., A. Bahloul, A. L. Wells, C. M. Yengo, C. A. Morris, H. L. Sweeney, and A. Houdusse. 2005. The structure of the myosin VI motor reveals the mechanism of directionality reversal. *Nature.* 435:779–785.

21. Volkmann, N., G. Ouyang, K. M. Trybus, D. J. DeRosier, S. Lowey, and D. Hanein. 2003. Myosin isoforms show unique conformations in the actin-bound state. *Proc. Natl. Acad. Sci. USA.* 100:3227–3232.

22. Volkmann, N., D. Hanein, G. Ouyang, K. M. Trybus, D. J. DeRosier, and S. Lowey. 2000. Evidence for cleft closure in actomyosin upon ADP release. *Nat. Struct. Biol.* 7:1147–1155.

23. Holmes, K. C., I. Angert, F. J. Kull, W. Jahn, and R. R. Schroder. 2003. Electron cryo-microscopy shows how strong binding of myosin to actin releases nucleotide. *Nature.* 425:423–427.

24. Song, L., H. Sweeney, and P. G. Fajer. 2006. Myosin cleft closure in muscle contraction. *Biophys. J.* 90:553a. (Abstr.)

25. Yengo, C. M., E. M. De La Cruz, L. R. Chrin, D. P. Gaffney 2nd, and C. L. Berger. 2002. Actin-induced closure of the actin-binding cleft of smooth muscle myosin. *J. Biol. Chem.* 277:24114–24119.

26. Zeng, W., P. B. Conibear, J. L. Dickens, R. A. Cowie, S. Wakelin, A. Malnasi-Csizmadia, and C. R. Bagshaw. 2004. Dynamics of actomyosin interactions in relation to the cross-bridge cycle. *Philos. Trans. R. Soc. Lond. B Biol. Sci.* 359:1843–1855.

27. Klein, J. C., A. R. Burr, M. A. Titus, and D. D. Thomas. 2006. Conformational heterogeneity in the Myosin II actin-binding cleft. *Biophys. J.* 90:312a. (Abstr.)

28. Rosenfeld, S. S., J. Xing, M. Whitaker, H. C. Cheung, F. Brown, A. Wells, R. A. Milligan, and H. L. Sweeney. 2000. Kinetic and spectroscopic evidence for three actomyosin:ADP states in smooth muscle. *J. Biol. Chem.* 275:25418–25426.

29. Robertson, C. I., D. P. Gaffney, L. R. Chrin, and C. L. Berger. 2005. Structural rearrangements in the active site of smooth-muscle myosin. *Biophys. J.* 89:1882–1892.

30. Sun, M., J. L. Oakes, S. K. Ananthanarayanan, K. H. Hawley, R. Y. Tsien, S. R. Adams, and C. M. Yengo. 2006. Dynamics of the upper 50 kDa domain of myosin V examined with fluorescence resonance energy transfer. *J. Biol. Chem.* 281:5711–5717.

31. Conibear, P. B., C. R. Bagshaw, P. G. Fajer, M. Kovacs, and A. Malnasi-Csizmadia. 2003. Myosin cleft movement and its coupling to actomyosin dissociation. *Nat. Struct. Biol.* 10:831–835.

32. Alessi, D. R., J. E. Corrie, P. G. Fajer, M. A. Ferenczi, D. D. Thomas, I. P. Trayer, and D. R. Trentham. 1992. Synthesis and properties of a conformationally restricted spin-labeled analog of ATP and its interaction with myosin and skeletal muscle. *Biochemistry.* 31:8043–8054.

33. Wilson, G. J., S. E. Shull, N. I. Naber, and R. Cooke. 1997. Myosin head interactions in Ca^{2+}-activated skinned rabbit skeletal muscle fibers. *J. Biochem. (Tokyo).* 122:563–571.

34. Weeds, A. G., and R. S. Taylor. 1975. Separation of subfragment-1 isoenzymes from rabbit skeletal muscle myosin. *Nature.* 257:54–56.

35. Spudich, J. A., and S. Watt. 1971. The regulation of rabbit skeletal muscle contraction. I. Biochemical studies of the interaction of the tropomyosin-troponin complex with actin and the proteolytic fragments of myosin. *J. Biol. Chem.* 246:4866–4871.

36. Karatzaferi, C., M. K. Chinn, and R. Cooke. 2004. The force exerted by a muscle cross-bridge depends directly on the strength of the actomyosin bond. *Biophys. J.* 87:2532–2544.

37. Thomas, D. D., and R. Cooke. 1980. Orientation of spin-labeled myosin heads in glycerinated muscle fibers. *Biophys. J.* 32:891–906.

38. Crowder, M. S., and R. Cooke. 1987. Orientation of spin-labeled nucleotides bound to myosin in glycerinated muscle fibers. *Biophys. J.* 51:323–333.

39. Rice, S., Y. Cui, C. Sindelar, N. Naber, M. Matuska, R. Vale, and R. Cooke. 2003. Thermodynamic properties of the Kinesin neck-region docking to the catalytic core. *Biophys. J.* 84:1844–1854.

40. Griffith, O. H., and P. C. Jost. 1976. Lipid spin labels in biological membranes. *In* Spin Labeling Theory and Applications. L. J. Berliner, editor. Academic Press, New York. 454–523.

41. Konrad, M., and R. S. Goody. 1982. Kinetic and thermodynamic properties of the ternary complex between F-actin, myosin subfragment 1 and adenosine 5′-[beta, gamma-imido]triphosphate. *Eur. J. Biochem.* 128:547–555.

42. Fisher, A. J., C. A. Smith, J. Thoden, R. Smith, K. Sutoh, H. M. Holden, and I. Rayment. 1995. X-ray structures of the myosin motor domain of *Dictyostelium discoideum* complexed with MgADP·BeF$_x$ and MgADP · AlF$_4^-$. *Biochemistry.* 34:8960–8972.

43. Chase, P. B., D. A. Martyn, and J. D. Hannon. 1994. Activation dependence and kinetics of force and stiffness inhibition by aluminiofluoride, a slowly dissociating analogue of inorganic phosphate, in chemically skinned fibres from rabbit psoas muscle. *J. Muscle Res. Cell Motil.* 15:119–129.

44. Regnier, M., P. B. Chase, and D. A. Martyn. 1999. Contractile properties of rabbit psoas muscle fibres inhibited by beryllium fluoride. *J. Muscle Res. Cell Motil.* 20:425–432.

45. Phan, B., and E. Reisler. 1992. Inhibition of myosin ATPase by beryllium fluoride. *Biochemistry.* 31:4787–4793.

46. Chinn, M. K., K. H. Myburgh, T. Pham, K. Franks-Skiba, and R. Cooke. 2000. The effect of polyethylene glycol on the mechanics and ATPase activity of active muscle fibers. *Biophys. J.* 78:927–939.

47 Fajer, P. G., E. A. Fajer, N. J. Brunsvold, and D. D. Thomas. 1988. Effect of AMPPNP on the orientation and rotational dynamics of spin-labeled muscle cross-bridges. *Biophys. J.* 53:513–524.

48. Pate, E., and R. Cooke. 1988. Energetics of the actomyosin bond in the filament array of muscle fibers. *Biophys. J.* 53:561–573.

49. Biosca, J. A., L. E. Greene, and E. Eisenberg. 1988. Binding of ADP and 5′-adenylyl imidodiphosphate to rabbit muscle myofibrils. *J. Biol. Chem.* 263:14231–14235.

50. Raucher, D., and P. G. Fajer. 1994. Orientation and dynamics of myosin heads in aluminum fluoride induced pre-power stroke states: an EPR study. *Biochemistry.* 33:11993–11999.

51. Malnasi-Csizmadia, A., J. L. Dickens, W. Zeng, and C. R. Bagshaw. 2005. Switch movements and the myosin crossbridge stroke. *J. Muscle Res. Cell Motil.* 26:31–37.

52. Naber, N., D. P. Gaffney, C. L. Berger, R. Cooke, and E. Pate. 2006. Conformational changes in the nucleotide pocket of smooth muscle myosin, measured with spin labeled nucleotides. *Biophys. J.* 90:553a. (Abstr.)

53. Trybus, K. M., and E. W. Taylor. 1982. Transient kinetics of adenosine 5′-diphosphate and adenosine 5′-(beta, gamma-imidotriphosphate) binding to subfragment 1 and actosubfragment 1. *Biochemistry.* 21:1284–1294.

54. Dantzig, J. A., Y. E. Goldman, N. C. Millar, J. Lacktis, and E. Homsher. 1992. Reversal of the cross-bridge force-generating transition by photogeneration of phosphate in rabbit psoas muscle fibres. *J. Physiol.* 451:247–278.

55. Kawai, M., and H. R. Halvorson. 1991. Two step mechanism of phosphate release and the mechanism of force generation in chemically skinned fibers of rabbit psoas muscle. *Biophys. J.* 59:329–342.